Calculation of Strength of Single-Lap Shear Specimen

Study shows that, in many cases, the AWS standardized model based on simple shear stress produces higher than actual tensile strength values for the brazed joint

BY E. LUGSCHEIDER, H. REIMANN AND O. KNOTEK

Introduction

Successful brazing not only depends on proper application of filler metals but also, to an essential degree, on brazement design. This includes the dimensions of joint clearance and overlap, as well as the selection of the base metals and filler metals. The design of brazed joints must be based on full knowledge of the parameters mentioned above and their influence on stress distribution after brazing and during the use of the brazed joint.

A predominant aspect of the theoretical and experimental description of joint strength is the condition where only tensile or shear forces act. This can be ensured simply by joining sheets in a single lap, which normally places the brazing filler metal under shear stress and, depending on the direction of the load, under tensile or compressive stress. By increasing the size of the lap, the ratio of the two types of stresses is shifted towards shear stresses. Practically, the stresses are decreased by increasing lap size and thickness of the sheets.

In the ideal case of shearing load within the joint, the shear stress within the brazing filler metal (τ) and tensile stress within the non-affected base metal (σ) are plotted against the overlap at the moment of fracture.

Paper presented at the Seventh International AWS Brazing Conference held in St. Louis, Missouri, during May 11-13, 1976

E. LUGSCHEIDER, H. REIMANN and O. KNOTEK are with the Institut fur Werkstoffkunde, Aachen, West Germany

Figure 1 shows the well-known graph according to Bredzs and Miller[1] with highest values of strength for the smallest overlap for the later discussed

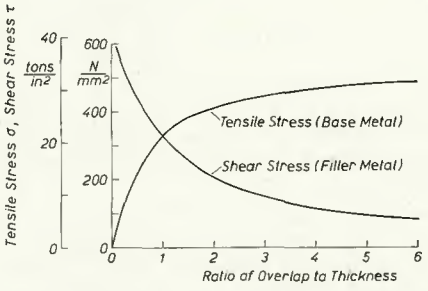

Fig. 1—Shear stresses and tensile stresses as a function of the ratio of overlap to thickness in a single lap specimen without consideration of bending. Type 316 stainless steel brazed with AWS BNi-2 filler metal at 1140 C (2090 F)

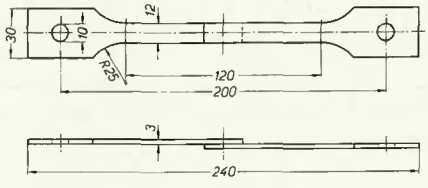

Fig. 2—Single lap shear specimen

filler-base metal combination (Table 1). Depending on the combination of the materials these values can be far above the yield strength of the base metals.

General Considerations

For the testpiece shown in Fig. 2, the ideal case of shear stress within the brazing filler metal has theoretical significance only. In most cases the stress situation is so complicated that it can be calculated only by an equivalent stress and the known theories of elasticity and plasticity. Tensile stress within the joint originates by twisting of the sample under load in the brazed area as shown in Fig. 3. Depending on the length of the overlap and the twisting angle, the tensile stress at fracture cannot be neglected. Therefore the case of ideal shearing should be compared with multi-dimensional stress conditions according to:

1. Mises criterion:[2]

$$\sigma_e^2 = \frac{1}{2}\left[(\sigma_I - \sigma_{III})^2 + (\sigma_{II} - \sigma_I)^2 + (\sigma_{III} - \sigma_{II})^2\right]$$

Table 1—Chemical Composition of Base Metal X 10 CrNiMoTi 18 10[a] and Filler Metal B Ni-2

	Ni	Cr	B	Si	C	Mn	Mo	Ti	Fe
X 10 CrNiMoTi 18 10	11.5	17.5	–	≤1.0	≤0.1	≤2.0	2.25	0.45	bal
B Ni-2	bal	7.0	3.1	4.5	–	–	–	–	3.0

[a]German alloy equivalent to Type 316 stainless steel

2. Beltrami-Huber hypothesis:[3]

$$\sigma_e^2 = \sigma_I^2 + \sigma_{II}^2 + \sigma_{III}^2 - 2\,\Omega\,(\sigma_I\,\sigma_{II} + \sigma_{III}\sigma_I + \sigma_{II}\,\sigma_{III}).$$

The equivalent stress σ_e is calculated on the principal stresses σ_I, σ_{II} and σ_{III} by both hypotheses. In our case σ_{III} will be neglected because it is very small in a single lap joint. Thus the three dimensional stress problem (stress in direction III originates by hindered cross contraction) will be reduced to a two dimensional one. The shear stress originating in the brazed joint continues in the overlapped base metal, and will be considered together with the stress component acting in the direction normal to it (Fig. 3).

On these premises and with a load distribution according to Fig. 3, the equivalent stresses can be calculated based on both hypotheses.

1.

$$2\,\sigma_e^2 = (\sigma_I - \sigma_{III})^2 + (\sigma_{II} - \sigma_I)^2 + (\sigma_{III} - \sigma_{II})^2$$

$$\sigma_{III} = 0$$

$$\sigma_I = \frac{p_I}{l \cdot b}\ ;\ p_I = p \cdot \cos\gamma$$

$$\sigma_{II} = \frac{p_{II}}{l \cdot b}\ ;\ p_{II} = p \cdot \cos\lambda = p \cdot \cos(90° - \gamma)$$

$$\sigma_I = \tau\ ;\ \sigma_{II} = \sigma$$

$$2\,\sigma_e^2 = \sigma_I^2 + (\sigma_{II} - \sigma_I)^2 + \sigma_{II}^2$$

$$2\,\sigma_e^2 = \sigma^2 \cdot \cos^2\gamma + \sigma^2 \cdot \sin^2\gamma - 2\,\sigma^2 \sin\gamma \cdot \cos\gamma + \sigma^2 \cdot \cos^2\gamma + \sigma^2 \cdot \sin^2\gamma$$

$$\frac{\sigma_e^2}{\sigma^2} = \cos^2\gamma - \sin\gamma \cdot \cos\gamma + \sin^2\gamma$$

$$\frac{\sigma_e}{\sigma} = \sqrt{1 - \sin\gamma \cdot \cos\gamma}$$

2.

$$\sigma_e^2 = \sigma_I^2 + \sigma_{II}^2 + \sigma_{III}^2 - 2\,\Omega(\sigma_I\,\sigma_{II} + \sigma_I\,\sigma_{III} + \sigma^{II}\sigma_{III})$$

$$\sigma_e^2 = \sigma_I^2 + \sigma_{II}^2 - 2\,\Omega\,\sigma_I\,\sigma_{II}$$

$$\sigma_e^2 = \sigma^2 \cdot \cos^2\gamma + \sigma^2 \cdot \sin^2\gamma - 2\,\Omega\,\sigma^2 \cdot \sin\gamma \cdot \cos\gamma$$

$$\frac{\sigma_e^2}{\sigma^2} = \sin^2\gamma + \cos^2\gamma - 2\,\Omega \cdot \sin\gamma \cdot \cos\gamma$$

$$\frac{\sigma_e}{\sigma} = \sqrt{1 - 2\,\Omega \cdot \sin\gamma \cdot \cos\gamma}$$

The results differ from each other by the factor 2 Ω* (Poisson ratio) of the trigonometric term under the root. For metallic materials Ω differs from 0.28 to 0.45. The upper limit Ω = 0.45 applies to high plastic deformation before and during the fracture and will be considered in the present case. Therefore the maximum difference results in 4.7% at a torsion angle of 45 degrees.

$$\frac{(\sigma_e/\sigma)\ \text{Mises}}{(\sigma_e/\sigma)\ \text{Beltrami, Huber}} = \frac{\sqrt{1 - \sin 45 \cdot \cos 45}}{\sqrt{1 - 0.9 \sin 45 \cdot \cos 45}} = 0.953$$

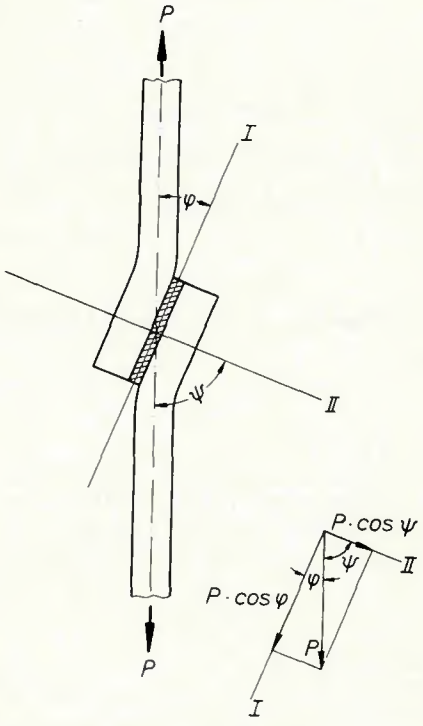

Fig. 3—Distribution of the load within the joint clearance of the single lap shear specimen

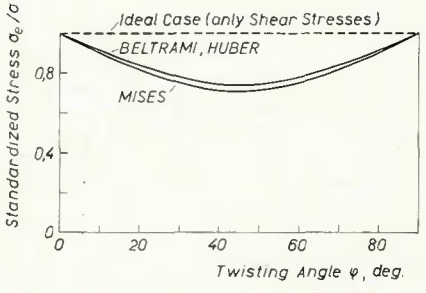

Fig. 4—Standardized stress σ_e/σ as a function of the twisting angle according to Mises and Beltrami-Huber criteria

Plotting the standardized stress (σ_e/σ) against the twisting angle (0-90 degrees), greater deviations result between the ideal shear stress (σ_e/σ = 1, γ = 0 degrees) and the calculated results of both hypotheses (Fig. 4). According to the Mises criterion the maximum deviation is 29.3% at a twisting angle γ = 45 degrees, and according to the Beltrami-Huber hy-

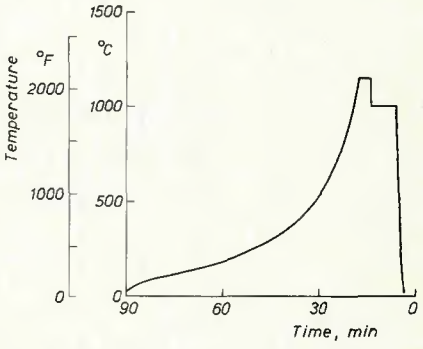

Fig. 5—Time-temperature cycle during brazing

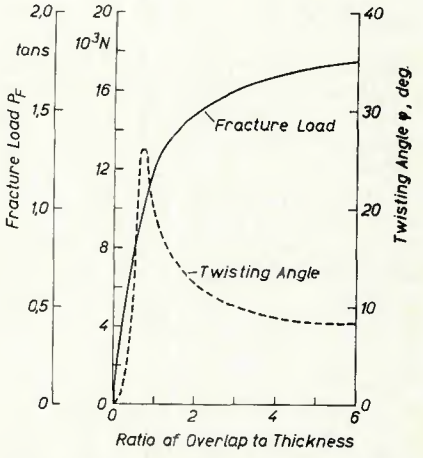

Fig. 6—Experimental values of fracture load and twisting angle as a function of the ratio overlap to thickness (see also Table 2)

Table 2—Actual Fracture Load P_F, Ratio of Overlap, Twisting Angle and Type of Fracture

No.	Ratio of overlap	Fracture load P_F N	tons	Twisting angle, deg	Type of fracture*
1	0.25	4248	0.426	1.883	1
2	0.375	5866	0.589	7.625	3
3	0.375	5572	0.559	8.450	3
4	0.375	5347	0.536	6.525	3
5	0.5	6543	0.657	13.275	3
6	0.75	11262	1.130	26.200	3
7	1.0	9378	0.941	17.975	3
8	1.0	12086	1.213	20.750	3
9	2.0	8986	0.902	12.275	3
10	6.0	17540	1.760	8.383	2

*For description of fracture types 1, 2 and 3, see text under "Experimental Work."

*Due to typesetting limitations, the lower case Greek character nu has been replaced by an upper case omega (Ω) in this report.

pothesis, 25.4%. Therefore, the strength of single lap joints calculated according to the simple shear stress model is too high in many cases and higher ultimate tensile strengths are pretended.

Experimental Work

In accordance with the AWS Standard Shear Test Method[4] single lap test, specimens made of stainless steel X 10 CrNiMoTi 18 10 (German Mat. Nr. 1.4571, similar to 316 stainless steel) and the filler metal BNi-2 (Table 1) were brazed with various ratios of overlap to thickness. All specimens were brazed under vacuum at 10^{-4} to 10^{-5} torr. The temperature cycle is shown in Fig. 5.

Figure 6 shows the results of the tensile tests. The actual fracture load P_F and the twisting angle γ are plotted as a function of the ratio of overlap to metal thickness. One can observe the steady increase of the fracture load to the maximum at a ratio of 6, and a maximum of the twisting angle of 26 deg in the ratio range 0.5 to 1. Note also that the twisting angle is small for both little and large overlap ratios. The observed values of P_F and γ used for Fig. 6 are shown in Table 2.

Three different kinds of fracture were observed:

1. Shear fracture in the brazed joint (twisting angle γ very small)
2. Fracture in the base metal, starting in the area of highest bending stress (twisting angle γ small to medium; hindered cross contraction and notch effect lead to additional local stress peaks)
3. Transition fractures between 1 and 2, above; crack starts in the base metal in the area of high bending stress and continues in the filler metal due to work hardening of the base metal by the bending.

As demonstrated in Fig. 4 the equivalent stress was calculated from the observed twisting angles at fracture. The equivalent stress was compared to ideal shear stress (Fig. 7). The largest deviation is found at the highest twisting angle which is associated with the overlap ratio of 0.75. The deviation is at least 19.72%, according to the Beltrami and Huber hypothesis and increases to 22.22% if the Mises criterion is applied. The fracture loads and twisting angles used for the calculation correspond to average values obtained by graphic means according to Fig. 6.

The plotting of shear and tensile stress in the filler metal, the tensile stress in the base metal and the resulting equivalent stress (calculated for the unfavorable case of Mises' criterion) in the filler metal with respect to the overlap ratio is shown in Fig. 8. This plot gives a result similar to Fig. 1. In addition, one can observe the size of the tensile stress within the joint. The maximum of the tensile stress corresponds with the highest value of the twisting angle γ and the minimum of the limit line (drawn fully in Fig. 8). The brazed joints seem to have their ultimate tensile strength in this range at remarkably low shear and tensile stresses.

However, this is contradictory to theoretical considerations. There should be a range of small overlap ratio in which the filler metal absorbs the main portion of stresses. Therefore, the fracture of the joint should occur there by reaching the shear yield strength. On the other hand the shear stresses decrease with increasing overlap ratio, and in the cross section of the base metal the tensile stress becomes more important. Hence within the range of transition fractures the tensile and shear yield strength are not reached, but a crack will be initiated by bending at the end of the overlap and exceeding the yield strength of the base metal. This crack continues within the filler metal of the joint.

Therefore the calculated values σ_e of the filler metal and σ of the base metal do not mean ultimate tensile strength. They are parts of the whole stress situation which causes the fracture.

At the minimum value of σ_e and σ a limit of overlap can be defined. Before this limit the actual fracture load is governed by the shear yield strength of the filler metal. If this limit is exceeded, the actual fracture loads are governed by the yield strength of the base metal (limit line of the hatched area in Fig. 8). The hatched area corresponds to the part of the whole stress situation which is not put into consideration by calculation, i.e., the stresses due to bending, notching and hindered cross contraction. Further considerations should deal with the real relations of stresses and working conditions.

Summary

The design optimization of a brazed system supposes an estimation of the stress distribution after brazing and during the use of the brazed joint. For a range of filler metal-base metal combinations, an attempt was made to determine stress distribution versus lap ratio using AWS standard single lap shear samples. The theoretical model of only shearing shows that the stress concentration is shifted by increasing overlap from the filler to the base metal. Normally the stress distribution is much more complicated, due to the torsion of the sample in the brazed area. This can be determined by calculation of an equivalent stress σ_e. In this paper it was shown that the standardized stress can deviate from the ideal case of pure shearing by as much as 29.3% at a twisting angle $\gamma = 45$ degrees. Therefore a higher than actual tensile strength of the brazed joint is simulated.

The brazed system of base metal (X 10 CrNiMoTi 18 10) and filler metal (B Ni-2) was investigated experimentally. The calculated standardized stress deviates in this case up to 19.7 or 22.2%. This occurs at the maximum torsion at the overlap ratio of 0.75. For the

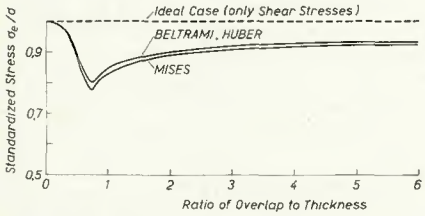

Fig. 7—Standardized stress σ_e/σ as a function of the ratio overlap to thickness calculated with the experimental determined twisting angles (see also Table 2). Twisting angle appears as γ in text

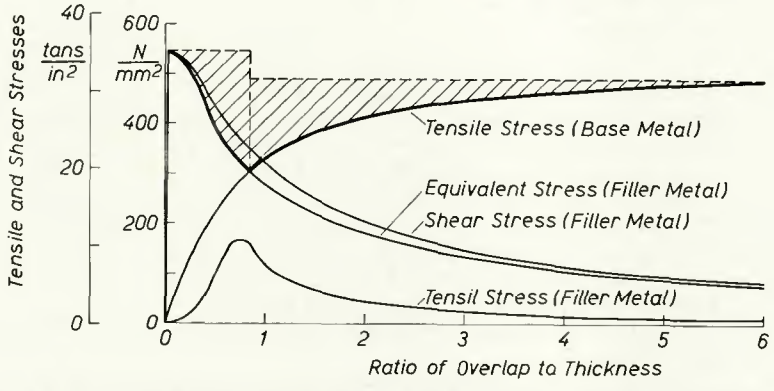

Fig. 8—Shear stresses, tensile stresses and equivalent stresses as a function of the ratio of overlap to thickness in a single lap specimen considering the torsion of the joint. Type 316 stainless steel brazed with AWS BNi-2 filler metal at 1140 C (2090 F)

chosen filler-base material combination the plotting of shear and of tensile stress in the filler metal, the tensile stress in the base metal, and the resulting equivalent stress depending on the overlap ratio, gives a result which is similar in principle to the models of Bredzs and Miller. But the type of fractures observed indicates that in the transition range, at small to medium overlap ratios, the cracks start in the base metal and continue in the filler metal. This is caused by local bending stress maxima which depend on the twisting angle and are amplified by the notch effect and hindered cross contraction.

References

1. Bredzs, N., and Miller, F. M., "Use of the AWS Shear Test Method to Evaluate Brazing Parameters," *Welding Journal*, 47 (11), Nov. 1968, *Res. Suppl.*, 481-s to 496-s.

2. Mises, R. V., Göttinger Nachr. mathem.-phys. Klasse, 1913, 582 to 592.

3. Beltrami, E., Rendiconti Lamb., 18 (1885), 704; and Huber, M. T., Czasopismo techniczne, Lemberg, 22 (1904), 81.

4. *Brazing Manual*, American Welding Society, Inc., Miami, Florida, 1963.

WRC Bulletin 213
February 1976

1. Weldability of Niobium Containing High Strength Low Alloy Steel
by J. Malcolm Gray

More recent development has extended the use of niobium strengthening to higher yield strengths, more complex base plate composition, greater thicknesses and to more severe climatic regions such as the Arctic. In addition, niobium contents have been increased (in some cases to above 0.10%), steel rolling and heat treating practices have become more sophisticated and welding evaluations are now concerned with all regions of the weld and adjacent base plate. The paper summarizes the extensive current usage of niobium strengthened steel in a wide variety of welded constructions.

2. A Review of the Structure and Properties of Welds in Columbium or Vanadium Containing High Strength Low Alloy Steels
by E. Levine and D. C. Hill

Recent publications concerned with welding of HSLA steels have concentrated on microstructural alterations of the ferrite-cementite phases (primarily ferrite) as being responsible for significant changes in toughness of both HAZ and weld metal properties after high heat input welding processes with high deposition rates such as submerged arc single and double pass welds.

Paper (1.) was sponsored by the Welding Research Council.

Paper (2.) was sponsored by the Weldability Committee of the Welding Research Council. The price of *WRC Bulletin 213* is $7.50 per copy. Orders should be sent with payment to the Welding Research Council, United Engineering Center, 345 East 47th Street, New York, NY 10017.

WRC Bulletin 214
April 1976

Stud Welding
by T. Shoup

Since the first practical application in the late thirties, arc stud welding has become an increasingly important joining process. The process was developed for the shipbuilding industry as a replacement for the time consuming drilling and through bolting to secure wooden decks to steel plates. During the past 30 years, the use of stud welding has become widespread in modern industry. Stud welding fasteners attached to one side of the workpiece can replace fasteners normally secured by riveting, drilling and tapping, manual arc welding, resistance welding or brazing. The process is one which permits wide latitude of welding techniques with assured satisfactory results. The application of arc stud welding has been widely accomplished with low-tensile strength steel fasteners. Other applications using aluminum and stainless steel materials and even titanium have been successful.

Publication of this paper was sponsored by the Interpretive Reports Committee of the Welding Research Council.

The price of *WRC Bulletin 214* is $6.50 per copy. Orders should be sent with payment to the Welding Research Council, United Engineering Center, 345 East 47th Street, New York, NY 10017.